System on Package (SoP) Millimeter Wave Filters for 5G Applications

Thesis by:

Jameel Showail

In Partial Fulfillment of the Requirements

For the Degree of

Master of Science

King Abdullah University of Science and Technology,

Thuwal, Kingdom of Saudi Arabia

May, 2018

EXAMINATION COMMITTEE PAGE

The thesis of Jameel Showail is approved by the examination committee.

Committee Chairperson: Dr. Atif Shamim

Committee Members: Dr. Khaled Salama, Dr. Thomas Anthopoulos

ABSTRACT

System on Package (SoP) Millimeter Wave Filters for 5G Applications

Jameel Showail

Bandpass filters are an essential component of wireless communication systems that only transmits frequencies corresponding to the communication band and rejects all other frequencies. As the deployment of 5G draws nearer, first deployments are expected in 2020 [1], the need for viable filters at the new frequency bands becomes more imminent.

Size and performance are two critical considerations for a filter that will be used in emerging mobile communication applications. The high frequency of 5G communication, 28 GHz as opposed to sub 6 GHz for nearly all previous communication protocols, means that previously utilized lumped component based solutions cannot be implemented since they are ill-suited for mm-wave applications.

The focus of this work is the miniaturization of a high-performance filter. The Substrate Integrated Waveguide (SIW) is a high performance and promising structure and Low Temperature Co-Fired Ceramic (LTCC) is a high-performance material that both can operate at higher frequencies than the technologies used for previous telecommunication generations.

To miniaturize the structure, a compact folded four-cavity SIW filter is designed, implemented and tested. The feeding structure is integrated into the filter to exploit the System on Package (SoP) attributes of LTCC and further reduce the total area of the filter individually and holistically when looking at the final integrated system.

Two unique three dimensional (3D) integrated SoP LTCC two-stage SIW single cavity filters and one unique four-cavity filter all with embedded planar resonators are designed, fabricated and tested. The embedded resonators create a two-stage effect in a single cavity filter. The better single cavity design provides a 15% fractional bandwidth at a center frequency of 28.12 GHz, and with an insertion loss of -0.53 dB. The fabricated four-cavity filter has a 3-dB bandwidth of .98GHz centered at 27.465 GHz, and with an insertion loss of -2.66 dB. The designs presented highlight some of the previously leveraged advantages of SoP designs while also including additions of embedded planar resonators to feed the SIW cavity. The integration of both elements realizes a compact and high-performance filter that is well suited for future mm-wave applications including 5G.

Table of Contents

LIST OF ABBREVIATIONS

CPW	Co-Planar Waveguide
IC	Integrated Circuit
LTCC	Low Temperature Co-Fired Ceramic
PCB	Printed Circuit Board
SIW	Substrate Integrate Waveguide
SoP	System on Package
TEM	transverse electromagnetic
TZ	transmission zero

LIST OF ILLUSTRATIONS

LIST OF TABLES

Chapter 1

1 INTRODUCTION

1.1 MOTIVATION

Filters are a well-researched topic which are necessary for the communications that we rely on daily. The over congestion of the sub 6GHz frequency range [2] has led to a scarcity of bandwidth in this range and limited room for future expansion. While some of the plans for 5G telecommunication are intended for sub 6 GHz, most of the plans for long-term usage involve the implementation at previously unutilized mm-wave frequencies. The most cited frequency is roughly 28 GHz, with slight shifts depending on the country [3]. There are no implemented filters with a reasonable size, insertion loss, and rejection at this frequency.

The need for compact and high-performance bandpass filters is a reflection of the devices that are becoming increasingly prevalent. Mobile telecommunication devices are ubiquitous and continue to swell in numbers. By most estimates, 30 billion devices will be connected by 2020 [4]. As 5G telecommunication systems are deployed to cope with the increasing demand, previous generations of telecommunications will continue to operate. A major reason for this is the high frequency of 5G signals which cannot travel as far as lower frequency signals. To ensure signal coverage in all areas, telecommunications carriers will combine high and low-frequency infrastructure [3].

The consequences are that modern mobile devices need to have an array of RF transceivers for all of the frequencies that they need to support. Other than supporting all generations of telecommunications infrastructure, devices also need capabilities such as Bluetooth, WI-FI, GPS, and potentially more. Since modern mobile devices are compact, the need for an additional system to be compact should be apparent.

The need for high-performance filters is more technical. Simply put, the filter is one of the earliest stages of a transceiver chain. Losses from the filter will propagate to all subsequent stages. When considering the Noise Figure of a whole system, a large Noise Figure in an early stage will increasingly affect each subsequent stage of the system negatively. The frequency of the filter dictates which technology is suitable for implementing a high-performance design. At low frequencies, active filters and lumped component filters are utilized. However, above 5 GHz active filters suffer from high losses and lumped component dimensions become on the order of the wavelength which renders them unusable. Thus, in the low mm-wave frequencies distributed transmission line filters are common due to their relative ease of production. As the frequency rises further, distributed filters also become impractical due to fabrication size limits in traditional PCBs and increased radiation losses. At these higher mm-wave frequencies, waveguide and SIW filters are employed as a solution when no other filters are practical.

1.1.1 Miniaturization through SoP

There are several approaches to miniaturizing mm-wave filters for compact solutions. For miniaturization in a practical application, the size of the entire system should be considered. The System on Package (SoP) is a recent design technique that incorporates several

components into one functional package. In a traditional Print Circuit Board (PCB), most components are individually fabricated and packaged as an Integrated Circuit (IC) which are then soldered to the PCB for final packaging. The IC components are packaged to connect the internal circuitry to conducting pads that will connect to the PCB. The packaging represents significant size waste since the packages are usually nonfunctional, i.e. their presence does not facilitate functionality other than interconnections and protection of the sensitive electronic circuitry.

In an SoP system, such as Low Temperature Co-Fired Ceramic (LTCC) designs, the material can be used to realize complex multilayer designs [5]-[7]. The SoP characteristic of LTCC makes it ideal for integration in compact devices. Continual improvements in the design constraints of LTCC has led to realizing increasingly miniaturized designs, such as [6] and [7]. LTCC provides the capacity for multi-layer traces and interconnections allowing for the implementation of Substrate Integrated Waveguide (SIW) cavities and interconnected planar designs. An SIW is a cavity formed by rows of vias in a substrate in place of solid metal cavity walls. The miniaturization of an SoP system come from not just the size reduction of individual components but also the miniaturization from reduced packaging.

1.2 OBJECTIVES AND CONTRIBUTIONS

The objectives of this work are as follows:

- Design a high-performance filter at 28 GHz for 5G applications. Particular attention should be paid to the insertion loss and the out of band rejection.

- Achieve significant size reduction for integration into a system by utilizing SoP designs. Reduction in size must be attained while the performance remains competitive to the literature.

1.3 CHALLENGES

The challenges faced in this work include:

- Improved roll-off and out-of-band rejection are usually attained by increasing the order of the filter. For a cavity filter, this means adding more cavities. This negatively impacts insertion loss, size, and cost.

- Cost of LTCC devices increases exponentially with the number of layers in the design. Odd ordered filters are easier to implement in a stacked LTCC design than even ordered filters because the input and output cavities are adjacent. However, odd ordered filters do not fully utilize the layers that used in the design. Since cavities are typically 3-5 LTCC layers, even ordered filters provide better rejection for the cost.

- Embedding a planar resonator in a cavity will change the field distribution of the cavity since fields do not exist within a conductor. The embedded resonators must be designed in conjunction with the cavity to ensure that their presence does not inhibit the desired resonance.

- Fabrication tolerances of LTCC include some shrinkage that cannot be perfectly predicted. Utilizing a design that embeds planar resonators into the cavity requires that the design is characterized for expected variation from fabrication.

1.4 PUBLICATIONS

1) J. Showail, M. Lahti, K. Kari, E. Arabi, P. Rantakari, I. Huhtinen, T. Vaha-Heikkila and A. Shamim, "SIW Cavity Filters with Embedded Planar Resonators in LTCC Package for 5G Applications", *in 2018 48th European Microwave Conference (EuMC), Madrid, 2018.*

2) J. Showail, M. Lahti, K. Kari, E. Arabi, P. Rantakari, I. Huhtinen, T. Vaha-Heikkila and A. Shamim, "Miniaturized Four-Cavity LTCC SoP Filter with Embedded Planar Resonators for 5G Applications", *IEEE Transactions on Microwave Theory and Techniques (MTT)*, 2018.

*submitted May, 2018.

Chapter 2

2 BANDPASS FILTER THEORY

2.1 INTRODUCTION

A filter is fundamentally a device which attenuates unwanted frequencies while allowing the desired frequencies to be transmitted unattenuated. There are four basic types of filters: lowpass, highpass, bandpass, and bandstop. Bandstop filters attenuates a specific stopband while transmitting frequencies that are both higher and lower than this stop band. A lowpass filter will only transmit frequencies that are lower than its cutoff frequency and a highpass filter operates in the opposite fashion. Bandpass filters will only transmit the frequencies that are in its passband, i.e. frequencies that are higher and lower than the passband will both be attenuated. Bandpass filters are essential to communication systems that are typically transmitted in a small frequency range. All other frequencies are not of interest and should be attenuated.

2.2 SCATTERING PARAMETERS

To measure the performance of RF devices scattering parameters (S-parameters) are often employed. S-parameter measurements do not require open or short circuit terminations to characterize a device. This simplifies the matter for high-frequency measurements. S-parameters can be thought of as a ratio of incident and either transmitted or reflected voltage. The measurement is conducted from both input and output ports for a total of four

parameters. (2.1) below is the matrix form of the S-parameters with the voltage defined with respect to each port.

$$\begin{pmatrix} V_1^- \\ V_2^- \end{pmatrix} = \begin{pmatrix} S_{11} & S_{12} \\ S_{21} & S_{22} \end{pmatrix} \begin{pmatrix} V_1^+ \\ V_2^+ \end{pmatrix} \tag{2.1}$$

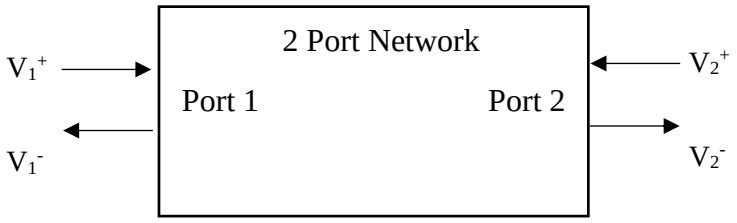

Figure 2.1: Model of voltages used for S parameters in two-port networks.

2.3 BANDPASS FILTER PARAMETERS

There are several values of merit used to evaluate the performance of filters. Often there are set specifications for each parameter that must be met for use in a specific application. An ideal bandpass filter will transmit the frequencies that are in its passband with no loss while completely rejecting all frequencies that are outside of the passband, i.e. the stopband. In practice, bandpass filters deviate from this ideal. The values of merit can describe how close the designed filter is to the ideal filter.

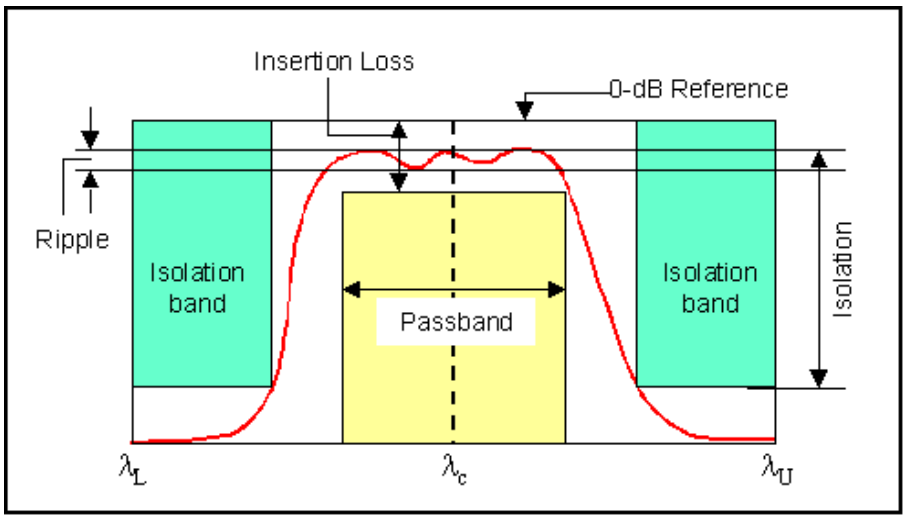

Figure 2.2: Illustration of bandpass filter response [8].

2.3.1 Frequency of operation

The frequency of operation is the center frequency of the passband. This is a critical parameter in the design of a filter; the center frequency determines that method for designing the filter. At low frequencies, active filters and lumped component filters are utilized. However, above 5 GHz active filters suffer from high losses and lumped components become on the order of the wavelength which renders them unusable. Thus, in the low mm-wave frequencies distributed transmission line filters are common due to their relative ease of production. As the frequency rises further, distributed filters also become impractical due to fabrication size limits in traditional PCBs. At these higher mm-wave frequencies, waveguide and SIW filters are employed as a solution when no other filters are practical.

2.3.2 Insertion loss

Insertion loss is one of the most important figures of merit in a bandpass filter. This is particularly true for filters that are part of a receiver chain. Since filters are usually one of the first stages of a receiver chain, loss at this stage will propagate through the entire system and negatively affect the noise figure at each subsequent stage. The quoted value of insertion loss is the minimum value, i.e. at the peak of the passband. Insertion loss is usually stated in dB and can be extracted from S21.

$$IL = -20\log(|S_{21}|) \tag{2.2}$$

Outside of the passband, insertion loss can be quoted as the out of band rejection. In that case, the stated rejection is a ceiling value that is not surpassed starting at a specified offset from the bandwidth. Good rejection is important to suppress unwanted frequencies. This is particularly important if the device is operating in a congested part of the frequency spectrum.

2.3.3 Bandwidth

The most commonly referred to bandwidth in filters is the 3-dB bandwidth. The 3-dB bandwidth includes frequencies that are within 3-dB of the peak insertion loss. Depending on the filter design, there may be a ripple in the passband before it curves down. If there is a ripple in the passband, it needs to be characterized and if possible minimized. A flat passband is closer to the ideal filter and is considered advantageous.

2.3.4 Return loss

Return loss is a measure of how much of the incident signal is reflected back. Equivalently, it is the in-band rejection from S11. Return loss is also stated as a ceiling value for the bandwidth. The matched bandwidth of the filter corresponds to frequencies where the return loss is less than -10 dB. If the 3-dB bandwidth is narrower than the matched bandwidth, the reported return loss is the peak value of S11 within the 3-dB bandwidth.

$$RL = -20\log(|S_{11}|) \tag{2.3}$$

2.3.5 Roll off

The roll off is a measure of how quickly the filter transitions from the passband to the stopband. As mentioned in the insertion loss section, the out of band rejection is a ceiling value starting at a specified offset from the passband. The roll off directly affects that offset from the passband. The area between the passband and the stopband is a transitional band where signals are neither fully transmitted or fully suppressed. A sharp roll off will shrink the transitional band and enable the specified rejection to occur near the passband. Whereas a gradual roll-off will have a large set of frequencies that are not part of the passband but are not suppressed in the filter.

2.4 CAVITY FILTER DESIGN

2.4.1 Resonant cavity

Resonant cavities are waveguides that are terminated on both ends with a conducting wall. A discussion on the benefits of waveguides is presented in chapter 4. A waveguide is a metal chamber that will internally reflect electromagnetic waves for transmission from one

end to another. Waveguides can be thought of as electrical plumbing that contains and transfer electromagnetic waves. They are realized as rectangular, cylindrical and spherical hollow metal tubes. The boundary conditions of Maxwell's equations dictate that there are no electromagnetic fields within a perfect conductor. This condition leads to total reflection of the wave off of a perfectly conducting surface. While waveguides are not made of perfectly conducting material, they are made with very good conductors where the conductor losses should be minimal.

Waveguides operate at certain frequencies corresponding to Transverse Electric (TE) or Transverse Magnetic (TM) modes. The modes of a waveguide are determined by (2.4).

$$f_{mn} = \frac{c}{2\pi\sqrt{\varepsilon_r}}\sqrt{\left(\frac{m\pi}{W}\right)^2 + \left(\frac{n\pi}{H}\right)^2} \tag{2.4}$$

For TM modes neither n nor m can be zero and for TE modes either one can be zero but not both allowed. Thus, the lowest order mode is the TE10 mode which corresponds to a half wavelength resonance with a maximum at the center and a minimum at the edges. Any frequencies that are below the lowest frequency mode cannot be transmitted through a waveguide. The lowest frequency mode is the cutoff frequency of a waveguide. It can be thought of as follows, frequencies that are lower than the cutoff frequency will have a longer wavelength and thus a half wavelength will not entirely fit in the dimensions of the waveguide.

A resonant cavity operates under the same principles as a waveguide. Placing a conductor on both ends of a waveguide transforms it into a resonant cavity. Similar to the other walls of the waveguide, the terminating conductor walls will reflect the electromagnetic waves back. This reflection means that at some wavelengths the wave will interfere constructively

with itself to create resonances. A resonance is when the waves introduced to the cavity form a standing wave. At resonant frequencies, the amplitude within the cavity is much greater than at other frequencies. Resonant frequencies of a cavity are determined by (2.5).

$$f_{res} = \frac{c}{2\pi\sqrt{\varepsilon_r}}\sqrt{\left(\frac{m\pi}{L}\right)^2 + \left(\frac{n\pi}{H}\right)^2 + \left(\frac{l\pi}{W}\right)^2} \tag{2.5}$$

2.4.2 Coupling matrix

Cavity resonators can have limited performance individually. A single cavity will exhibit a filter like response at its resonance frequencies with excellent insertion loss. However, the roll-off or bandwidth may not be up to the specifications of the application in question. To improve both bandwidth and roll-off multiple resonant cavities can be employed. This comes at the cost of insertion loss due to the longer transmission path of the waves. This trade-off is well known and limits the order of a cavity filter for practical reasons.

When there are multiple cavities in a cavity filter, the first cavity is the input cavity and the last cavity is the output cavity. The feeding structure will couple with these cavities to transmit and receive the signal at the ports. However, for the wave to travel between the input and output cavities the other cavities in the filter need to be excited as well. Internal excitations of a cavity filter are through apertures in the conductor separating two cavities.

The coupling matrix is an $N \times N$ matrix where N is the number of cavities in the filter. Each field of the matrix indicates the mutual coupling between two corresponding cavities. The matrix is symmetrical along the diagonal axis since the coupling between cavities one and four, for example, is the same as the coupling between cavities four and one. There are two important attributes to the values in the coupling matrix, the magnitude and the sign.

The sign indicates the type of coupling which determines the placement of the coupling slots. The magnitude determines the size of the coupling slots. There are two types of coupling; the basic principle of coupling is to create slots where the field distributions are identical. Positive coupling is also known as magnetic coupling. Conversely, negative coupling is known as electric coupling. As the naming suggest, positive coupling is the result of a slot at a position of maximum H field. Accordingly, negative coupling is the result of a slot at a position of maximum E field. A position of maximum E field is a position of minimum H field and vice versa.

$$\begin{bmatrix} 1 & M_{12} & M_{13} & M_{14} \\ M_{21} & 1 & M_{23} & M_{24} \\ M_{31} & M_{32} & 1 & M_{34} \\ M_{41} & M_{42} & M_{43} & 1 \end{bmatrix}$$

The most common mode in cavity resonator and filters is the TE101 mode since it is the fundamental, lowest frequency, mode of the cavity. The field distribution of a cavity in the TE101 mode corresponds to an E field maximum at the center of the cavity and the H field maximums at the edges of the cavity. As such, inducing positive coupling between two cavities requires a coupling slot near the sidewall of the cavity. This can be realized as either slots in the sidewall of two horizontally adjacent cavities or as slots in the metal wall separating two vertically stacked cavities. Negative couple requires a coupling the center of the cavity. therefore, the only way to realize negative coupling between two cavities is a slot in the in the center of the metallic cavity wall separating two vertically stacked cavities.

2.5 SIW THEORY

2.5.1 Transmission lines

Transmission lines are a fundamental concept to microwave components. Transmission lines are two conductors that support the propagation of a Transverse Electromagnetic (TEM) wave to transmit an electrical signal over relatively long distances with as minimum loss as possible. Examples of transmission lines include microstrip lines, CPW lines, stripline, and coaxial cables.

2.5.2 Waveguides

Waveguides are not strictly considered transmission lines because they are formed of one conductor instead of two and thus do not support the propagation of TEM waves. However, waveguides can propagate TE or TM waves to transmit an electrical signal. In fact, waveguides have the distinct advantages of lower loss and high-power handling capabilities. This makes them appealing to applications where those factors are important, such as defense and satellite related systems. Additionally, waveguides exhibit low loss at much higher frequencies than integrated transmission lines. This makes waveguides an ideal candidate for mm-wave transmission where planar transmission lines would suffer loss from the radiation and the dielectric. Waveguides also have the distinct disadvantage of being bulky and needing lengthy transitions to be integrated with the rest of the system circuitry. Further, waveguides will not propagate waves that are lower than the cutoff frequency of the waveguide. This cutoff frequency is entirely determined by the dimensions of the waveguide. For low-frequency applications, this requires a very large waveguide (30 cm^2 for an air filled with a cutoff of roughly 1 GHz).

2.5.3 SIW

Substrate Integrated Waveguides (SIW) offer a beneficial compromise between waveguides and integrated transmission lines. SIWs are formed by placing a conductor layer entirely covering both sides of the substrate and connecting those metal layers with a row of vias where the sidewall of the waveguide should be. When the spaces between the sidewall vias are small compared to the wavelength, the row of vias acts similar to a solid metal sidewall. (2.7) characterizes the difference in dimensions between a waveguide and an SIW by considering the via size and spacing in the effective dimensions of the SIW. The integration of the waveguide in the substrate reduces the need for lengthy transitions to the waveguide. An SIW can be formed in the same substrate that contains other circuitry for a more compact design.

The SIW can be thought of as a dielectric filled waveguide. The dielectric filling of the SIW allows for more compact dimensions than a traditional air-filled waveguide. Another factor that arises with a dielectric filling is the tangent dielectric loss. For traditional PCB materials, the tangent loss is roughly 0.03 to 0.3 [9] and increases with frequency. Therefore, mm-wave applications in PCB SIWs suffer from high insertion loss. However, high-performance materials, such as LTCC with a dielectric loss of <0.002 until 100 GHz, circumvent this design constraint for mm-wave applications. It is no surprise, therefore, that SIWs made with high-performance materials are often the method of choice for recent mm-wave designs.

2.6 SIW CAVITY RESONATOR

When a waveguide is terminated on both ends with metallic walls it becomes a cavity resonator. At resonant frequencies, the waves reflect off the metal walls and interfere constructively. This results in a low loss resonance at frequencies that correspond to the resonant modes of the cavity. A cavity resonator can also be implemented in an SIW with a row of vias for the terminating metal walls. Cavity resonators are the best performing resonators at mm-wave frequencies. Planar resonators result in losses that are too high at mm-wave frequencies.

The resonances of an SIW cavity are determined by (2.6). This is similar to (2.5), which characterizes the resonances of a solid metal wall cavity.

$$f_{res} = \frac{c}{2\pi\sqrt{\varepsilon_r}}\sqrt{\left(\frac{m\pi}{L_{eff}}\right)^2 + \left(\frac{n\pi}{H}\right)^2 + \left(\frac{l\pi}{W_{eff}}\right)^2} \tag{2.6}$$

Where L_{eff} is the effective length of the cavity, W_{eff} is the effective width of the cavity, H is the effective height of the cavity, c is the speed of light, and ε_r is the relative permittivity. Since the cavity has via walls instead of solid walls, there needs to be coa rrection to determine each dimension's effective size. To account for the effective length and width of the cavity, the dimensions are measured from the center of the innermost row of vias then corrected with (2.7). The same equation is used to calculated the effective width, where D is the diameter of the sidewall vias and p is the pitch between adjacent vias.

$$L_{eff} = L - \frac{D^2}{.95p} \tag{2.7}$$

Chapter 3

3 BACKGROUND AND LITERATURE REVIEW

3.1 5G FILTERS

While the implementation of 5G is rapidly approaching, there is still a need for much of the infrastructure that will eventually allow for the next generation of telecommunications. To date, the number of filters specifically designed for 5G bands that have been implemented has been limited, with only [10] - [12] to the author's knowledge. Important practical shortcomings of these designs are high insertion loss (>4 dB) and large device footprint respectively. These examples illustrate two of the largest issues that arise with mm-wave filters. Periodic waveguide filters offer the best solutions for insertion loss, such as [12], but the size of waveguide filters is not realistic for mobile applications. CMOS integrated filters are the smallest realizable filters. However, the measured insertion loss from the active filters at this frequency range is between 4.1-7.5 dB [10] [11]. The importance of high performance and compact filters is outlined in the motivation section.

3.2 SOP MINIATURIZATION AND INTEGRATION OF MM-WAVE SIW FILTERS

SIW cavity filters are a compromise between the insertion loss and the size of the fabricated filter. In recent years there have been some mm-wave SIW cavity-based filters in multilayer technology such as LTCC [13]-[16]. One advantage with multilayer technologies is the ability to stack cavities for a folded SIW cavity filter. Most LTCC cavity

filters are either third order or fifth order. The reason for why filters with an even number of cavities are not realized is explained in the Four cavity filter section of this paper. The performance of mm-wave SIW filters has propelled recent research to utilize the SIW structure for filters, particularly in conjunction with high-performance materials such as LTCC and Rogers.

3.2.1 LTCC

LTCC is a multilayer technology that allows metal traces on the layers and vias as interconnections between the layers. The LTCC material is a high-performance dielectric with excellent performance in the mm-wave range. The exact specifications of the LTCC material depend on the type of LTCC used and the fabrication limitations are dependent on the LTCC foundry. The fabrication process for an LTCC design involves punching the holes for the via, filling those vias, and screen printing conductors for the metal traces on each layer. Then the layers are aligned and co-fired together below 1000°C to create a single device. The process is illustrated in Figure 3.1.

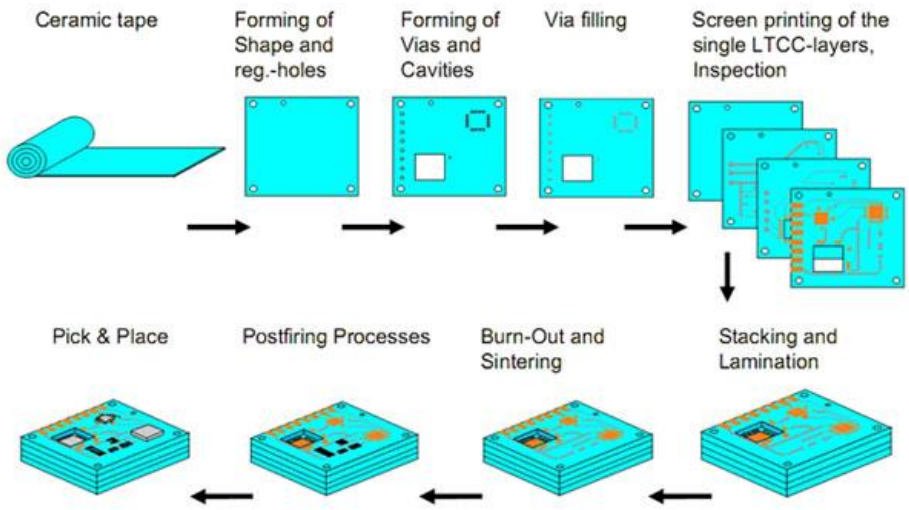

Figure 3.1: LTCC fabrication process [28].

The capabilities of LTCC have facilitated several recent 3D multilayer designs that are miniaturized compared to their planar counterparts. LTCC supports the 3D miniaturization of lumped components and the miniaturization of SIW cavity structures by stacking the cavities.

3.2.2 Filter order

The SIW cavity filters achieve improved size as compared to a periodic waveguide structure because the cavities can be vertically stacked. In a filter with an odd number of cavities, there are two side by side cavities from the top of the device until the lowermost cavity. The bottom cavity is placed in the center and there is only one cavity in those layers. Realizing an odd ordered filter is not cost effective in LTCC because cost rises exponentially with the number of layers. And since cavities are usually composed of three to five layers, adding layers for a vertically stacked cavity should be justified with as much performance gain as possible. The only four-cavity SIW filter near 28 GHz is [13]; the

transitions to the cavities are larger than the four cavities in this design. Figure 2.1 depicts the filter from [13] from which it is apparent that filter area is not utilized efficiently.

An attempt to remedy the issue mentioned above is presented in [20], where a transition is made for the signal from the bottommost layer to the top of the device. While this does alleviate the cost related issues associated with adding more layers for another cavity, it comes at the cost of larger area and increased loss from the lengthy transitions. In this work, another approach is presented as a solution to designing a cavity filter with an even number of cavities. A four-cavity filter is then designed and fabricated as an example of the design.

3.2.3 Feeding structure integration

The need for integrated filters in a compact system is a design consideration that influences the designed feeding structure. Feeding structures can significantly impact size and performance of an SIW filter. In general, a more gradual the transition between the cavities and the remaining circuitry will yield better performance. Abrupt changes in impedance perceived by the transmitted waves cause more of the signal to be reflected back. This, as expected, lowers the performance of the filter. Thus, there is a design trade-off between size and performance to consider for an SIW filter.

Often the feeding structure extends beyond the cavities. In some publications, this addition to the size from the feeding structure is not quoted. In [16] the CPW pads and part of the microstrip feed are not included in the quoted size of the of the filter. This additional size can be difficult to estimate. In [17] the full size is documented; the feeding structure is a relatively short addition to the cavity and still increases the total area by over 50%. As presented in the previous chapter, four cavity filters cannot be fed from the same side if all

of the cavities are operating at the TE101 mode which can lead to a transition besides the cavity from the bottommost layer to the top. However, in [13] the reported four cavity filter has lengthy test leads. Including the test leads in the size of the filter would more than double the reported area. The feeding structure must be considered in the size of a filter that will be integrated into remaining circuitry for an accurate estimate of the spatial impact.

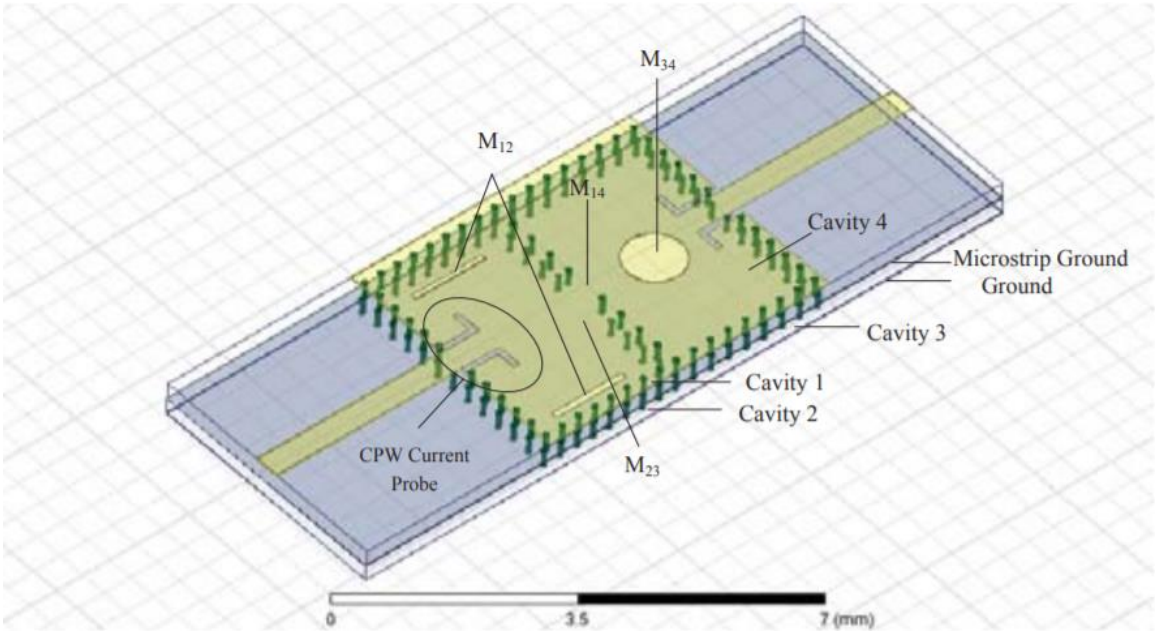

Figure 3.1: Model of the four-cavity LTCC filter from [13].

To circumvent the issue of increased size due to the feeding structure some multilayer designs will stack the feeding structure vertically above the cavity. This results in no increase in the area of the filter. The stacked compact feeding structure comes at the cost of an additional layer of the substrate and potentially worse insertion loss. A comparative study of SIW cavity feeding techniques in [18] discusses feeding by open circuit microstrip coupling, short-circuited microstrip, and via probe excitation. The findings indicated that

there are differences in insertion loss, return loss, and bandwidth between all three feeding techniques. Additionally, the introduction of the vias as excitation probes slightly reduces the size of the cavity by the induced dipole moment from the probes [19]. The best insertion loss was achieved by the open circuit microstrip coupling through a slot. However, the probe excitation achieved similar insertion loss, roughly 10% worse, and better bandwidth, return loss, and size. The bandwidth is roughly 20% larger and the return loss is roughly 10% better.

The above-mentioned feeding structures are often used for odd ordered SIW cavity filters. In an odd ordered filter, the feeding structure can be placed vertically stacked above the cavity and thus not increase the area of the device. In an even ordered filter, such as a four-cavity filter, the input and output cavities are not horizontally adjacent. This configuration requires additional area beyond the cavities for one of the feeding structures to transition to the layer of the output cavity. There are no mm-wave four-cavity filters with a compact SoP feeding structure in the literature.

Chapter 4

4 PROPOSED SOP CAVITY FILTERS

4.1 SINGLE CAVITY FILTERS

4.1.1 Feeding structure and embedded planar resonators

The cavity is chosen as the basic structure to build upon due to their high performance. In the single cavity filter and the input cavity of the four-cavity filter, using (2.6), $m = 2$, $n = 0$, and $l = 1$. This is the lowest frequency mode in the cavity since the center post suppresses lower frequency resonance. The post at the center of the cavity acts as an electrical wall and prevents the TE101 mode from resonating in the cavity [21]. This is done such that the electric field that is formed in the cavity does not interfere with the one induced from the planar stripline resonators.

In this case, the via size and spacing is set to the minimum allowable dimensions by the LTCC design rules. The diameter of the vias is 80µm and their pitch is 160µm. Two and three via rows were simulated to explore the effect on insertion loss. Further, both a staggered (triangle lattice) and an unstaggered (square lattice) design was explored through simulations. The result was that the staggered design with three via rows produced a better insertion loss. This is contrary to the observations noted in [22], where a square lattice produced slightly better results. One possible reason for this difference is that when the vias are staggered in this the design, the via rows are brought closer together to take advantage of the staggering while maintain the 160µm pitch.

To exploit the multilayer capabilities of LTCC a planar resonator is embedded into the cavity structure. Typically, a filter is either designed as a planar filter composed of distributed components or as a cavity filter built upon cavities. However, since the LTCC SIW cavities are filled with multiple layers of the substrate, a planar component can be embedded into the cavity. This unique design strategy significantly affects the frequency response of the cavity filter. Figure 4.1 depicts an initial cavity design that has only a via as a feeding structure and no embedded resonators. The frequency response of the empty cavity with the same dimensions of the final designs is two distinct and small resonances instead of joining to create a wider bandwidth or sharper roll-off.

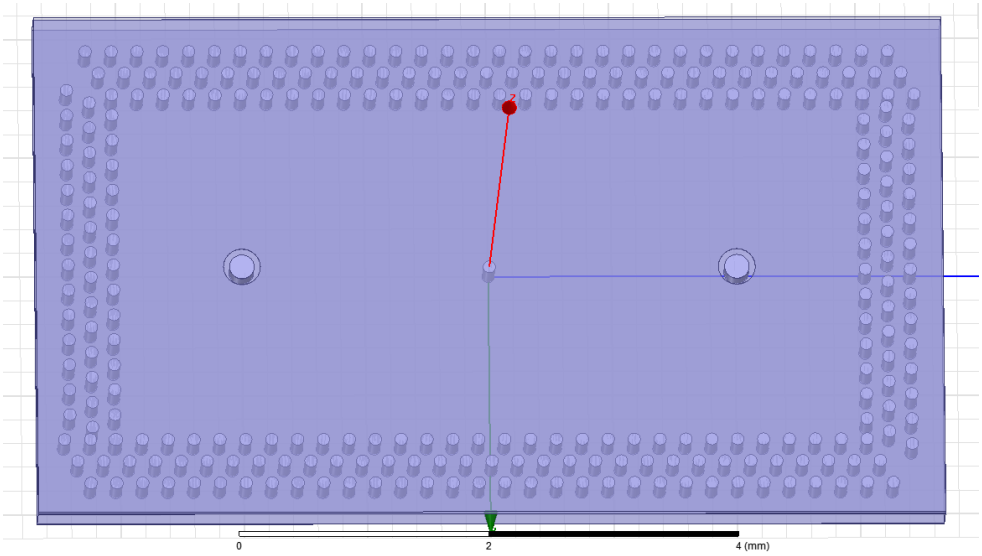

Figure 4.1: initial cavity design with via feed and no embedded resonators.

The cavity is made of four layers of LTCC with the embedded planar resonators placed in the middle layer. The feeding structure has an electrical length of roughly λ/4 and the stripline resonator has roughly the same electrical length. Therefore, there is a surface current maximum at the end of the stripline resonator at its resonant frequency. The induced electric field from the planar resonator is produced near the feed via at the desired

frequencies. Thus, by placing the post at the center of the cavity, the resonate cavity electric fields will be in the same location as planar resonator electric fields. This is apparent in Figure 4.3 where (a) is the resonance from the stripline and (b) is the TE201 cavity resonance.

The size of the metallic post at the center of the cavity affects the frequency of the resonance induced by the stripline. As the diameter of the center post increases, as does the resonant frequency. There is no documentation, to the author's knowledge, of this effect. Since the post acts as an electrical wall, a wider post is a wider electrical wall which makes the effective size of the cavity smaller. This effect is simulated and graphed in Figure 4.2.

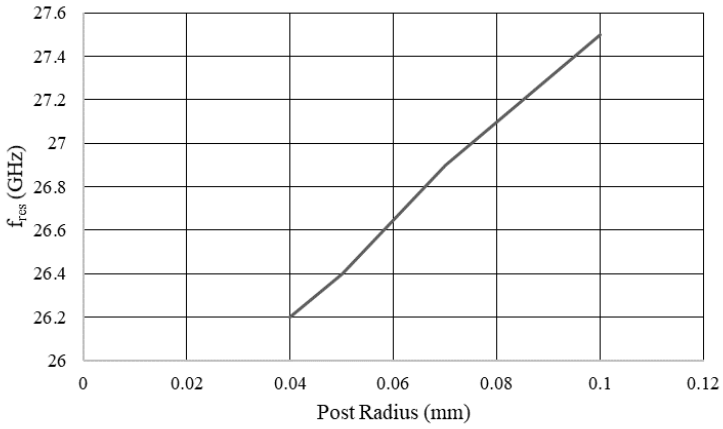

Figure 4.2: Graph of the stripline induced resonance versus the radius of the center post in the center-fed stripline design.

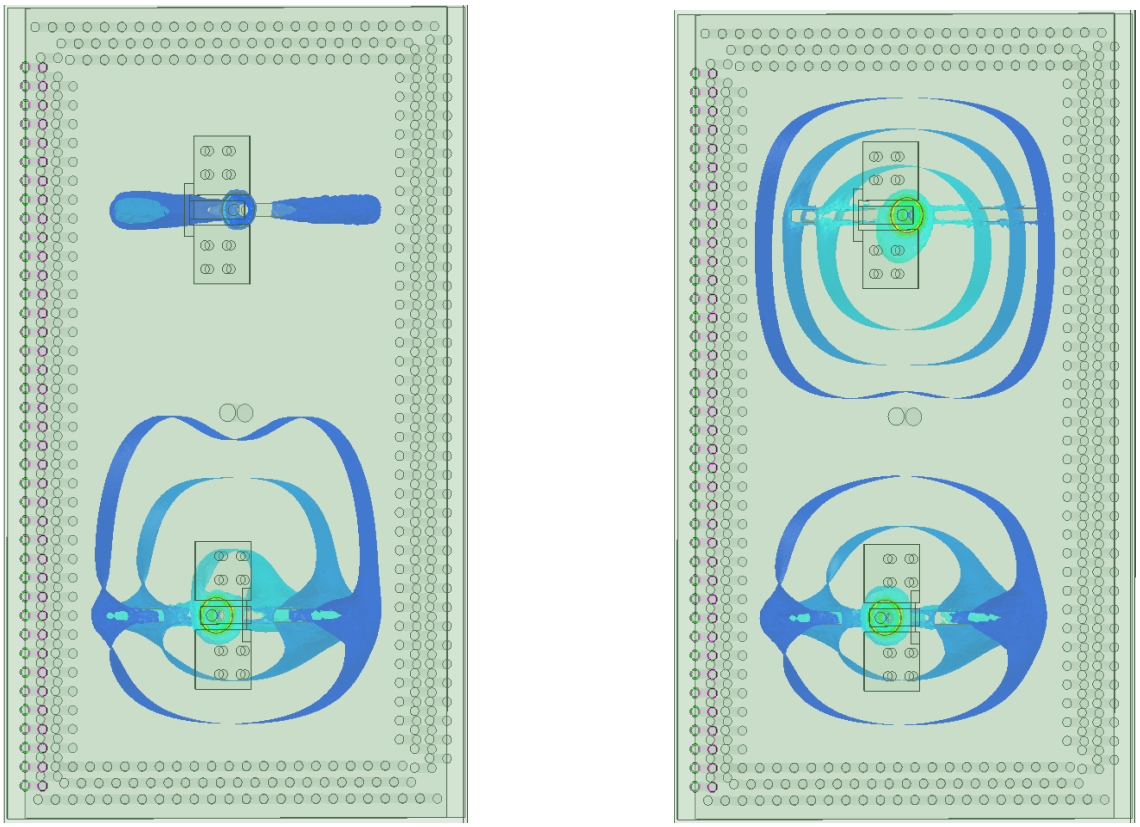

(a) (b)

Figure 4.3: E field plots of the two resonances in the passband of the center-fed stripline single cavity filter. (a) 27 GHz and (b) 28.9 GHz.

The cavity feeding structure is made up of three stages. All three stages are designed to have a characteristic impedance of 50 Ohms for low loss transitions. The first stage is a Co-Planar Waveguide (CPW) used for the initial excitation. CPW is an ideal connection for probing and integration on to a Printed Circuit Board (PCB). The second stage is a via that is connected from the signal trace of the CPW to the middle layer of the cavity, i.e. it is only present in the top two layers of the four-layer cavity. Based on the results in [22], the via is placed λ/4 away from the cavity edge and thereafter optimized. This value is the feeding via offset in Table 1. This via alone is enough to excite the cavity, although not

enough to create a second order effect in a single cavity filter; the third stage is added for the second resonance to achieve a wider bandwidth and better rejection. The feeding CPW and via are together initially set to have an electrical length of λ/4. The third stage is a stripline that is connected to the second stage via. The stripline is initially set to λ/4 and thereafter optimized. The open stub length (OSL) of the design is calculated from the end of the feeding via to the edge of the stripline. In the center fed stripline design, the value represents half of the total stripline size.

Optimization of the feeding structure must be done while considering all three stages. If the embedded planar resonator is a symmetrical stripline transmission line then the second stage feeding via will always be the same size, i.e. from the top surface to the middle of the cavity. Thus, the length of the surface CPW and the embedded stripline resonator should be optimized together to ensure the total electrical length of the feeding structure is the desired λ/2. Table 1 contains the final dimensions for both designs.

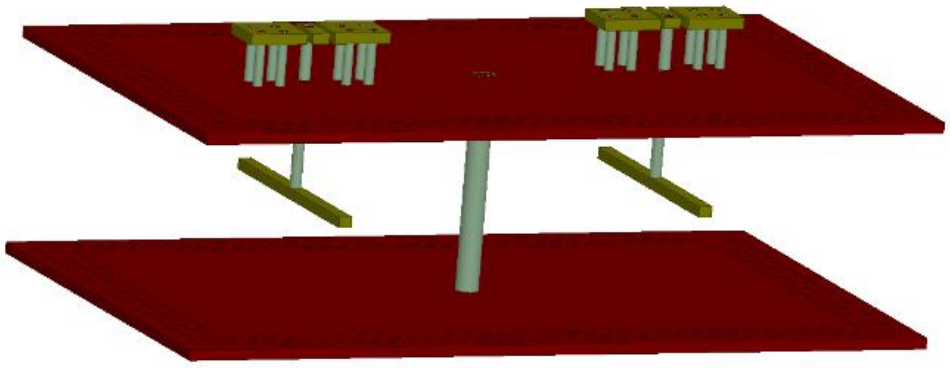

(a)

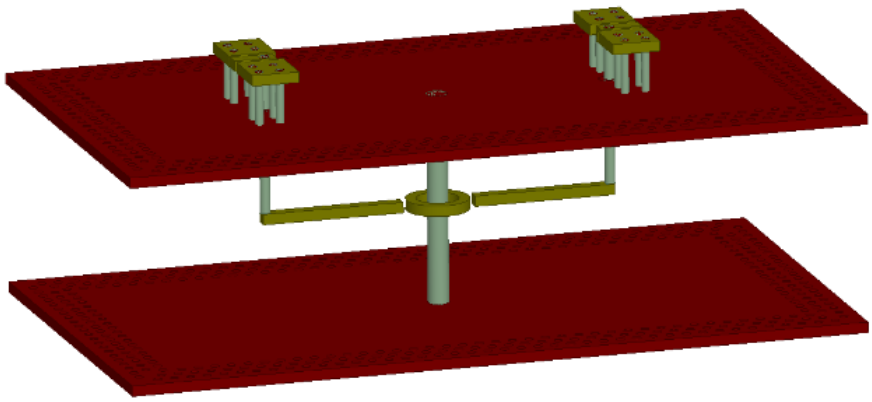

(b)

Figure 4.4: Exploded view of the single cavity filters with embedded planar resonators. (a) View of the filter with the center-fed stripline resonator in the cavity and (b) the design with a stripline ring around the cavity's center post. Note that the sidewall vias are excluded from both to view the interior of the cavity.

There are two planar designs at the center of the cavity included in this paper. Figure 4.4 has an exploded view of both for illustration. The first novel design has the feeding via connected to the center of a roughly λ/2 stripline. This can increase the bandwidth and improve the rejection. The two designs have different sized cavities (3.01 x 5.82 mm and 2.9 x 6.1 mm respectively) with nonproportional side lengths. Additionally, the striplines within the cavity, as well as the feeding structure, are rotated such that the stripline lies upon the center of the E field pattern when looking at the top of the filter. This also means that the feeding offset value in the center fed stripline design is measured as the distance from the longer side of the cavity. This dimension is also measured from the center of the innermost sidewall via.

Initially, the design with a center fed stripline had the embedded resonator oriented along the length of the cavity, as in the second proposed design. However, the field distribution and shape were more affected by the resonator being oriented along the length of the cavity. The field distribution at resonance is plotted for both designs in Figure 4.5.

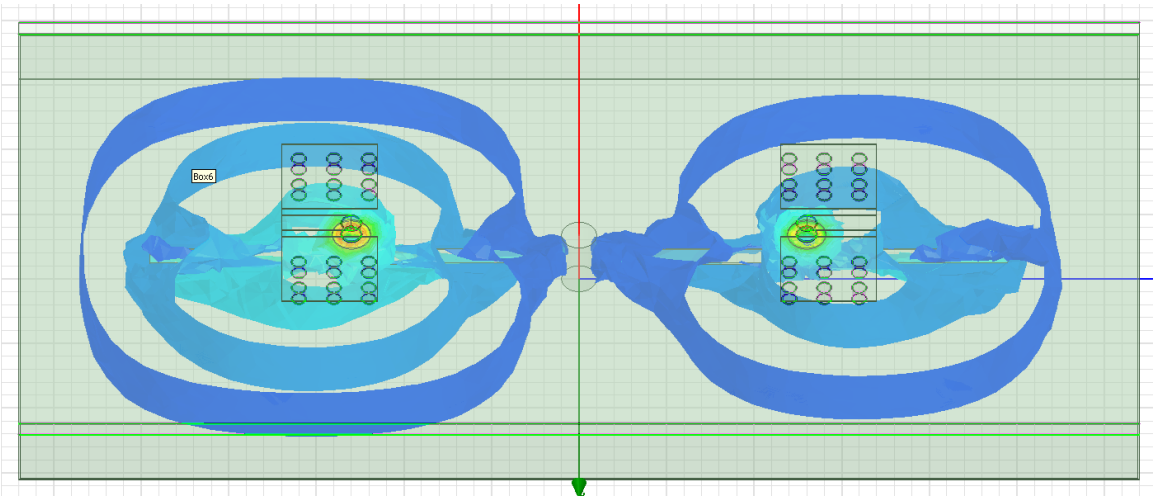

(a)

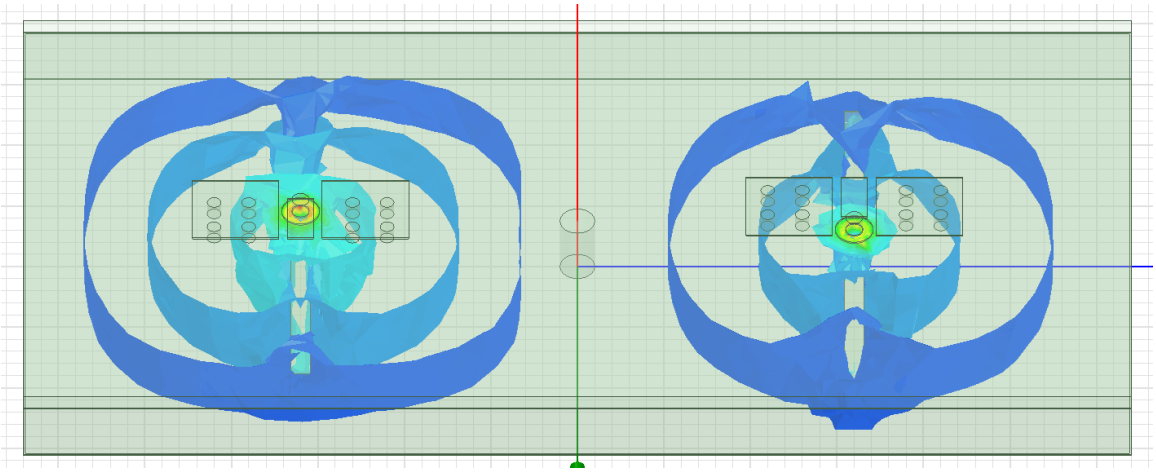

(b)

Figure 4.5: Comparison of two orientations for the embedded center fed stripline resonators

The second design has a stripline originating from the feeding via and terminating just 50 μm from an embedded stripline ring. The stripline ring was initially introduced as a ring resonator with the intention that it would resonate at a similar frequency as the cavity. However, during simulations, it was discovered that when the ring is much smaller than what is necessary for a 28GHz resonance, another resonance is introduced. Analysis of the fields in simulations revealed that when the ring is small and close to the center post, it allows fields to either terminate at the center post or at the edge of the ring. This second resonance widens the bandwidth of the filter compared to an empty cavity.

TABLE I

Dimensions of parameters for both single cavity designs

Parameters	**Design**	
	Design with ring (mm)	**Center fed stripline design (mm)**
Cavity length	6.1	5.82
Cavity width	2.9	3.01
Cavity height	0.368	0.368
Sidewall via diameter	0.08	0.08
Sidewall via pitch	0.16	0.16
CPW length	0.3	0.366
OSL	1.35	1.15
Center post diameter	0.15	0.15
Feeding via offset	1.08	1.24
Ring diameter	0.6	N/A

*Cavity dimensions are measured from the center of the innermost sidewall via.

4.1.2 Fabrication and measurements

The filters have been fabricated at VTT Finland using LTCC Ferro A6M-E tape system with a final fired layer thickness of roughly 93µm, a loss tangent of <0.002 (1-100 GHz), and a dielectric constant of 5.7 +/- 0.2 (1-100 GHz). The system utilizes screen-printed Au conductors (FX30-025JH) with the conductivity of ~7 x 106 S/m and estimated conductor thickness of 4-7 µm. The top layer was printed with 400 mesh screen meanwhile the non-critical layers were printed with 325 mesh screen. The via holes were mechanically punched and then filled with CN30-078 Au paste using stencil-printing. The tape layers were aligned using registration holes in the sheets and stacked in the mechanical fixture. The lamination was carried out isostatically and eventually co-fired at a maximum temperature of 855 °C.

The final device is constructed from five layers of LTCC, four layers for the cavity and one layer to feed the filter. Figure 4.6 shows a top view of the fabricated filters where GSG pads feeding the cavity filters can be seen. The dimensions of the final product are 4.44 x 7.55 x 0.47 mm. This final product is ready for integration in its current package. In total, 4 LTCC panels were fabricated. The tolerance of the xy-dimensions is ±0.2%.

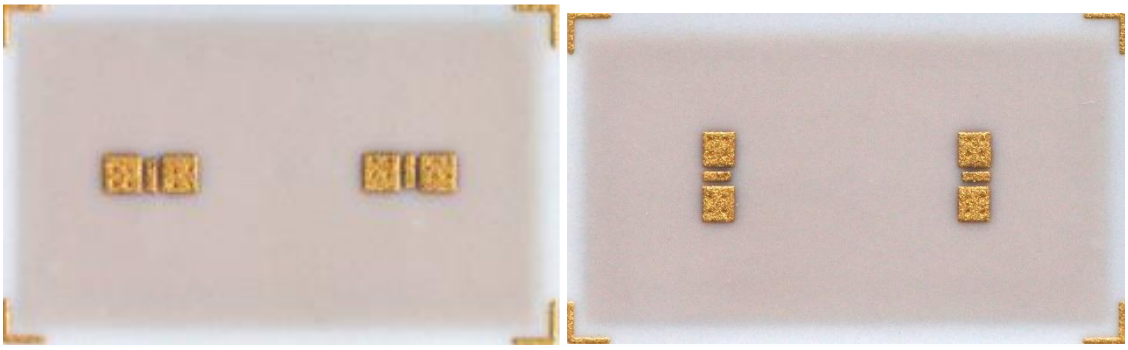

(a) (b)

Figure 4.6: Top view of fabricated single cavity filters with GSG pads visible. (a) The center fed cavity design and (b) the design with a ring near the center post. Note that the input port orientation varies due to design differences

Figure 4.7 shows the simulated and measured results for the two filters. The S-parameter measurements were conducted using a network analyzer and on-wafer setup on a probe station. The network analyzer was calibrated using on-wafer calibration standards with load-reflect-reflect-match (LRRM) calibration method.

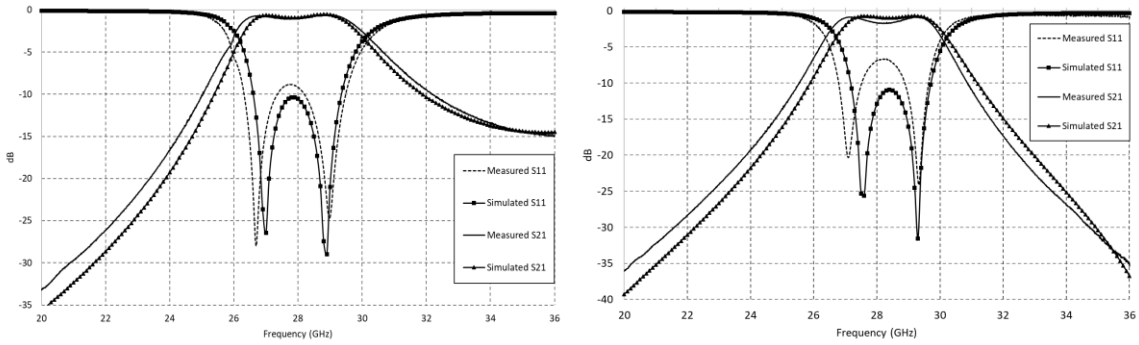

(a) (b)

Figure 4.7: Simulation and measurement results for both single cavity filters with embedded planar resonators. (a) The design with center-fed stripline resonator and (b) the design with a metal ring around the center post.

The design with a center fed stripline produced a 3-dB bandwidth of 4.29 GHz. This corresponds to a 15% fractional bandwidth with a center frequency of 28.12 GHz. The minimum insertion loss in the passband is -0.53 dB, measured at 28.84 GHz. There is a slight ripple in the passband but is as expected from the simulation results. The passband ripple is 0.58 dB. There are very subtle differences between the simulation and measurement results. Again, the lower frequency resonance of the two in-band resonances

is shifted. However, the shift is much less in this case and only widens the bandwidth of the filter further. The return loss is again higher than expected due to the resonance shift but the difference is less than in the other design.

The second design with a ring around the center post of the cavity had a measured 3-dB bandwidth of 3.72 GHz. This corresponds to a 13% fractional bandwidth with a center frequency of 28.21 GHz. The minimum insertion loss within the passband is -0.82 dB, measured at 29.33 GHz. There is a ripple of less than 1 dB in the passband of the measured results. The simulation yielded a smaller ripple in the passband. The disagreement between the measured and simulated results can be attributed to the shift in the lower frequency resonance of the two in-band resonances. The other result of this shift is that the measured maximum return loss is noticeably larger than in the simulations. From the results, the second design is more susceptible to frequency shifts due to fabrication limitations and is thus implemented as a four-cavity filter.

4.2 FILTER ORDER AND MUTUAL COUPLING IMPLEMENTATION

The coupling matrix details the electromagnetic interactions between stages of a filter. In the case of cavity filter, this interaction is between the cavities. There are multiple configurations for the coupling matrix which dictate the shape of the S21 curve. In addition, the magnitude of the coupling parameters depends on the intended return loss for the bandwidth. The magnitude of the coupling parameters is determined by the size of the coupling slots. The placement of the coupling slots determines the sign of the coupling between the cavities. The signs of the coupling matrix are responsible for the number and placement of transmission zeros.

For a fourth order cavity filter, with a transmission zero on both sides of the passband, there is positive coupling between cavities 1 &2, 2&3, and 3&4. However, there is negative coupling between cavities 1 and 4, i.e. the input and output cavities respectively. The coupling matrix is illustrated in Figure 4.8. Positive coupling is realized with a slot at a position with an H field maximum (E field minimum). This field position is near the cavity walls. Therefore, positive coupling can be realized with either slots in the sidewall of two horizontally adjacent cavities or as slots in the metal wall separating two vertically stacked cavities. Negative couple requires a coupling slot a position of with an H field minimum (E field maximum). This occurs at the center of the cavity if it is operating at the TE101 mode. As such, the only way to realize negative coupling between two cavities is a slot in the metallic cavity wall separating two vertically stacked cavities.

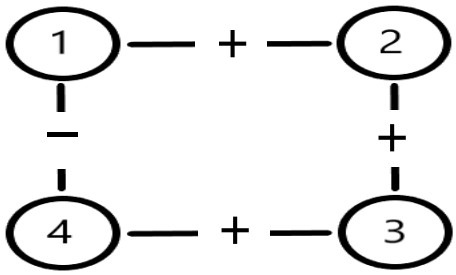

Figure 4.8: A simplified coupling matric for a four-cavity filter with a transmission zero on both sides of the passband.

For an odd ordered filter with a transmission zero on both sides of the passband, there is positive coupling between the input and output cavities. This permits the input and output cavities to be horizontally side by side. Horizontally adjacent input and output cavities reduce the complexity of feeding structures because there is no need for lengthy transitions besides the cavities to excite one of the ports.

4.3 FOUR-CAVITY FILTER

4.3.1 Practical Design Considerations

Due to the negative coupling between the input and output cavities, the standard design for a fourth order filter (with a TZ on both sides of the passband) requires the input and output cavities to be vertically stacked. While this is realizable in LTCC, having the input and output on opposite sides of the filter creates a lot of difficulty for testing and integration. As such most implementations of LTCC cavity filters are either third or fifth order filters, such as [14] [15]. The limitations to designing an effective and efficient feeding structure for a four-cavity filter stem from that fact that designs usually have all four cavities operating at the same mode. The TE101 mode is the fundamental mode of the cavity. It the most commonly used mode in resonators. If all four cavities are operating at the TE101 mode then the vertically stacked cavities cannot be offset to offset the input. For the negative coupling between the input and output cavity, operating at the TE101 mode, there needs to be a slot at the maximum E field position, i.e. the center of both cavities. If the centers of the cavities need to be in line and they are the same size then they must have the same position. In a cavity that is operating at the TE201 mode, there are two positions of maximum E field in the cavity; this is apparent in the E field plots on the single cavity filter in Figure 4.3. This fact is exploited to feed the input cavity at one E field maximum and couple with the output cavity at the other E field maximum. Thus, to offset the input and output, the first cavity is forced to operate at the TE201 mode.

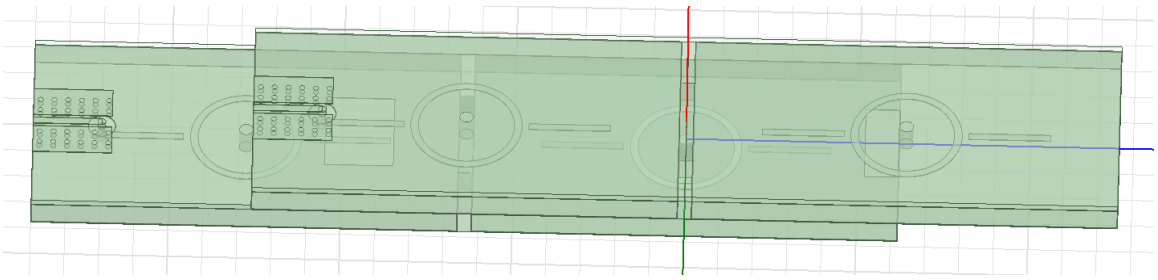

Figure 4.9: Initial four cavity filter with all cavities in TE201 mode and embedded resonators in every cavity.

Initial designs of the four-cavity filter had all four cavities operating the TE201 mode. This was done such that the modes of all of the cavities would be the same. And since all of the cavities are operating in the TE201 mode, there are two E field maximums in all of the cavities for added design flexibility. However, the results and characteristics of the filter required a redesign of the filter. By designing all of the cavities to be in the TE201 mode, the total size of the filter increases. And the increased propagation length within the dielectric material caused by the larger filter results in more insertion loss. Additionally, the planar resonators were designed to be excited by a port. Their presence without an excitation port results in no gain to the filter performance and a degradation of the standing waves within the cavity. Thus, to alleviate all of these issues while maintaining the staggered input on the same side, only the input cavity is designed to be in the TE201 mode.

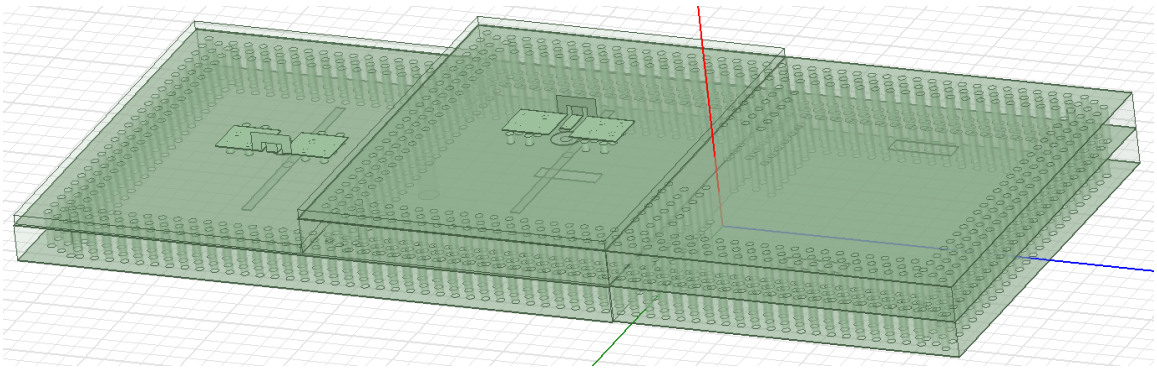

Figure 4.10: Earlier design of four-cavity filter with the input and output on different layers

The first SIW four-cavity filter with only one cavity operating in the TE201 mode and the remaining cavities operating in the TE101 is displayed in Figure 4.10. It is apparent from the figure that the input and output cavities are on different layers. This presents a problem for probing for testing and is problematic for integration onto a flat PCB.

To suppress the TE101 mode in the first cavity there is a metallic post placed at the center of the cavity, as in the single cavity filter. Since the TE201 mode operates at a higher frequency than the TE101 mode in the same cavity, if two cavities are to resonate at the same frequency but different modes then would need to be different sizes. The cavity operating at the TE201 mode would need to be larger than the cavity operating at the TE101 mode such that the resonances coincide at the same frequency. The larger first cavity allows the input feed to be positioned at the center of one of the resonances in the input TE201 without going through the output TE101 cavity. The field positions of the resonance opposite the feeding structure interact with the other three smaller, operating in the TE101 mode, cavities as expected in the coupling matrix.

The input cavity is a different size from the other three cavities. This is because the input cavity is operating at a different mode than the other three cavities. The three cavities that

are the same size are all operating at their fundamental mode, TE101. The input cavity is operating at the mode TE201 in the passband. The dimensions of the cavities are chosen such that the only overlapping resonance is in the passband. This helps create a wide rejection region outside of the passband. As in the single cavity filter presented in this work, the input cavity has a center post to suppress the TE101 mode and facilitate the cavity to operate in the TE201 mode.

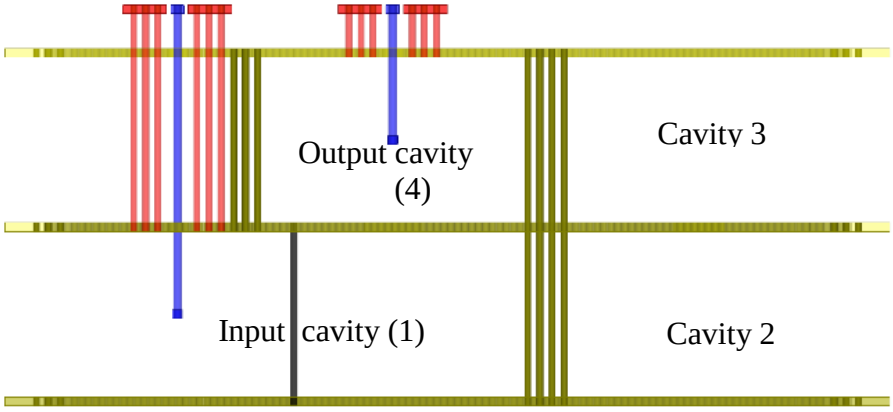

(a)

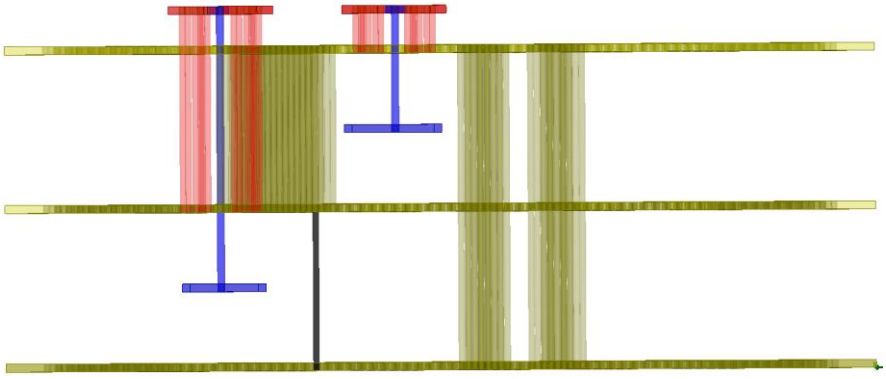

(b)

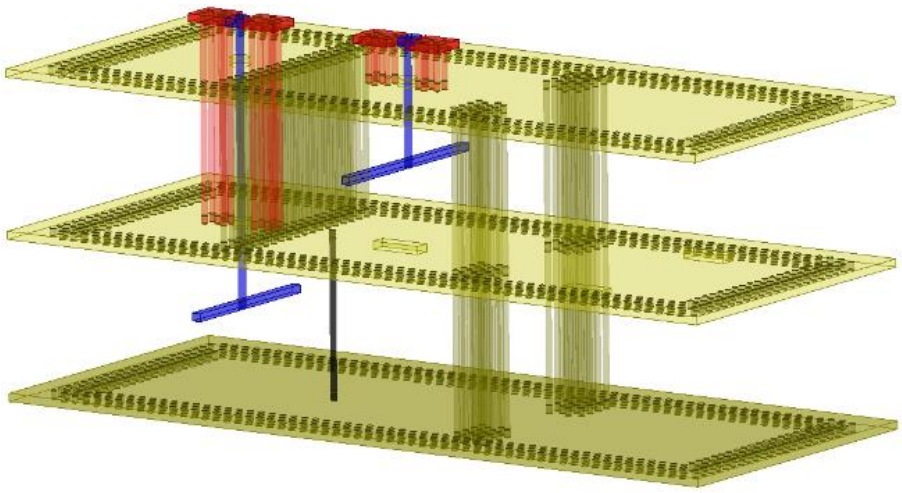

(c)

Figure 4.11: A 3D exploded view of the final four-cavity filter with the outer ring of sidewall vias omitted. (a) Side view, (b) angled view and (c) other angled view.

Further, as in the single cavity filter, the feeding structure together with the stripline resonator are designed to resonate near the cavity resonance. In the final design, the input and output ports are placed on the same layer to alleviate the aforementioned issues associated with the ports being on different layers. This is done by extending the feeding via for the input cavity. This is apparent in Figure 4.11. Since the feeding via that connects the stripline resonator to the surface CPW line is different sizes for the input and the output, the stripline resonator is different lengths in the two cavities. The input feeding via is longer and thus the stripline resonator in the input cavity is shorter to compensate for this difference. Additionally, the grounding vias for the CPW ground extend below the uppermost ground plane. The dimensions of the gap between the grounding vias and the signal via are set such that the signal is transmitting on a 50 Ohm transmission line. This is to ensure that the signal has a well-matched transmission line up to the cavity.

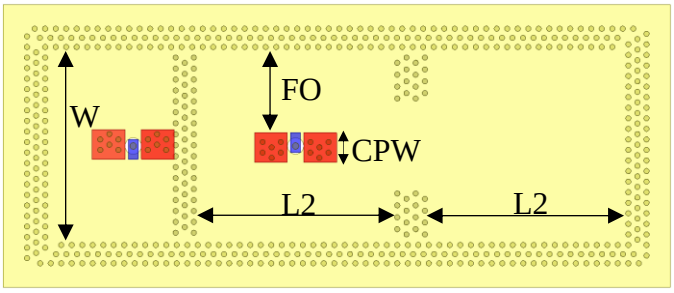

(a)

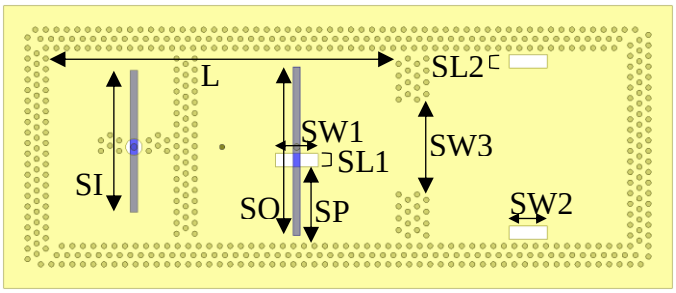

(b)

Figure 4.12: Dissection of the filter to show parameters. (a) view of metal layers 8 and 9. (b) view of metal layers 2, 4 and 6, layers 2 and 6 only have the input and output stripline resonator respectively.

TABLE II

Dimensions of Parameters for the Four- Cavity Filter

Parameters	**Dimensions (mm)**
W	3.0
L	5.36
L2	3.1
FO	1.3
CPW	0.45

Parameters	Dimensions (mm)
SI	2.15
SO	2.55
SP	1.2
SW1	0.65
SL1	0.2
SW2	0.58
SL2	0.2
SW3	1.52

4.3.2 Results

The four-cavity filter was also fabricated at VTT Finland with the same process and LTCC Ferro A6M-E tape system as the single cavity filter. The filter has a measured 3-dB bandwidth of .98 GHz. This corresponds to a 3.6% fractional bandwidth centered at centered at 27.45 GHz. This is a wider bandwidth than the simulated .89 GHz. In addition, the bandwidth center is shifted 0.53 GHz from 27.98 GHz. The minimum measured insertion loss is -2.66 dB measured at 27.44 GHz. This is nearly the exact same as the simulated insertion loss, which was -2.69 dB. The measured matched return loss bandwidth is .77 GHz centered at 27.37 GHz. The simulated matched return loss bandwidth is .78 GHz centered at 27.93 GHz. Comparing the results of the four-cavity filter to the single cavity filter, the out of band rejection is significantly better in the four-cavity filter. While the measured results are slightly worse than the simulated, the measured S21 still does not rise above -30 dB outside of the passband. In the lower stopband, the measured S21 rejection is better than -30 dB at a 0.44 GHz offset from the passband and in the upper stopband it is better than -30 dB at a .75 GHz offset. This corresponds to an average roll

off of 49 dB/GHz. In simulations, this out of band rejection is attained at least between 20 and 40 GHz.

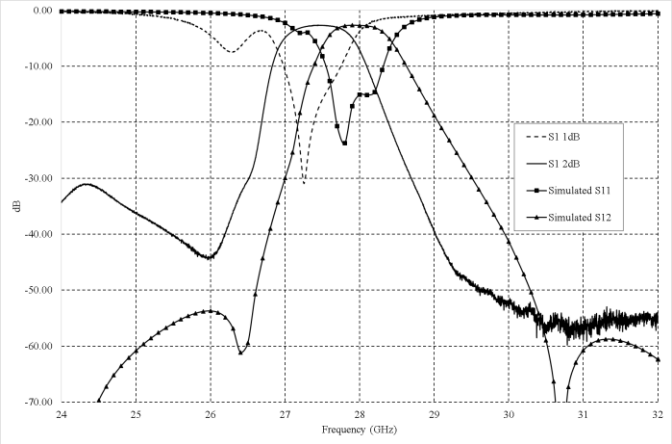

Figure 4.13: Simulated and measured S parameters for the four-cavity filter.

4.3.3 Post Measurement Simulations

One of the final modifications to ensure that the design is fabricable was to increase the size of the apertures that allowed the feeding vias to connect to the stripline resonator. In these simulations the internal aperture to cavity 1 was not enlarged. This was noticed after the measured results exhibited an out of band dip in S11. Updating the simulations to reflect this enlarged aperture resulted in the same shape in the simulations as the measured results. This does not affect the results significantly because the dip in S11 is small and the filter is not matched outside of the passband. Slight dimensional changes in the design make it possible to realize the desired frequency response with the enlarged apertures.

To determine the cause of the roughly 0.5 GHz shift in the passband of the filter a post-fabrication analysis of the devices was conducted. The post-fabrication analysis revealed a larger than shrinkage in the vias and the surface metals. Shrinkage in the surface metals

leads to expansion of the apertures slots in the metal. The surface metals shrank roughly 10%, which is an acceptable threshold and does not affect the results significantly. The shrinkage in the vias was larger than expected and larger than the shrinkage in the surface metals. The sidewall vias were measured at 75% of their punched size. This shrinkage causes the effective dimensions of the cavity, characterized by (2.7), to increase. The larger effective cavity resonates at a lower frequency. A possible cause of this higher than expected via shrinkage is the density of the sidewall vias. The sidewall via pitch was designed to be at the minimum allowable separation in the LTCC fabrication guidelines. In the post-fabrication analysis, the sidewall via shrinkage was determined by dicing the device near the via sidewall. The shrinkage of the single center metallic post was determined in post simulations to be less than the sidewall via shrinkage. This supports the notion that a less dense concentration of sidewall vias would result in less via shrinkage. Compensating for both shrinkages resulted in well-matched transmission results between the post simulations and the measurements, displayed in Figure 4.14.

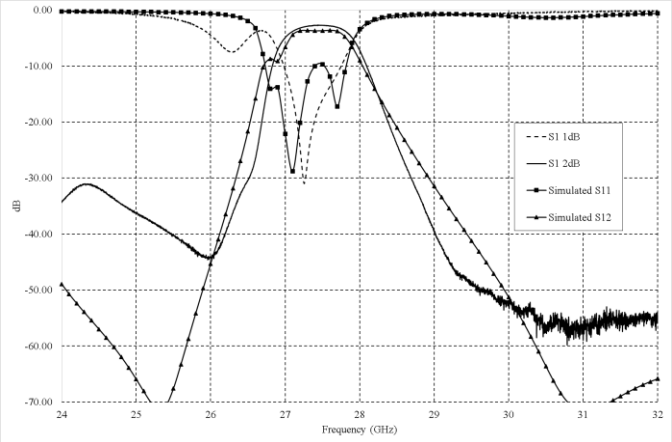

Figure 4.14: Post measurement simulations and measured results for the four-cavity filter.

4.4 COMPARISONS WITH LITERATURE

The four-cavity filter is realized in 9 layers of LTCC, 4 layers per cavity and one layer to place the CPW ports. The importance of a folded four-cavity filter for size and cost-effectiveness is explained in the Literature Review section of this paper. The presented work is compared to other cavity filters designed near 28 GHz in the literature. Size and insertion loss are the most important characteristics to consider for a mobile telecommunications filter. This work is significantly smaller than all other SIW filters except [13]. However, the lengthy transitions of [13], whose length had to be estimated, likely contribute to the additional 1 dB of loss despite also utilizing LTCC Ferro – A6M. The filter in [13] is the only other folded four-cavity design near 28 GHz.

As mentioned in the Literature Review section of this paper, there is a tradeoff between how gradual the transitions to the cavities are and the impact to insertion loss from the transitions. It is apparent from the comparison table that the integration of the feeding structure above the cavities does not significantly affect the insertion loss. The loss resulting from the SoP integrated feeding structure is less than the insertion loss of the single cavity filter, which is roughly .5 dB.

The most significant factor to the size reduction is the 3D design of the folded four-cavity filter. The design limitations with the feeding structure, as discussed in the Four-Cavity Filter section of this chapter, along with technological limitations prevent the realization of compact four-cavity filters. Stacked cavities are only possible in a small number of multilayer SoP technologies. If the filter is designed using a standard PCB substrate then

the filter is usually a series of horizontally adjacent cavities. The final result is a filter that occupies an unrealistic footprint for a mobile device.

Another important factor for consideration in a filter is the roll-off and the out-of-band rejection. The significance is the suppression of undesired frequencies. A sharp roll-off translates into frequencies near the passband being attenuated adequately. And a good out-of-band rejection means that undesired frequencies that are not immediately near the passband are heavily attenuated. The proposed four-cavity filter has one of the best roll-off and out-of-band rejections. When considering the rejection in conjunction with size, the much larger size of the filters that have better rejection does not merit their improvements in rejection.

TABLE III

Comparison with other SIW mm-Wave Filters

Work	**Tech.**	**Order**	**Size (mm^2)**	**IL (dB)**	**BW (GHz)**	**Avg. Rejection @ 2 GHz Offset (dB)**	**Avg. Roll-off (dB/100 MHz)**	**f_c (GHz)**
This work	LTCC	2	33.5	0.53	4.29	17.2	0.47	28.1
This work	LTCC	4	43.5	2.66	0.98	43.8	4.9	27.45
[13]	LTCC	4	~55	3.2	1.5	29	0.7	28.25
[21]	PCB	2	229	3	~1	25	1.2	35.8
[23]	Rogers	4	81	3.6	3.75	23	0.8	29.4
[24]	Air filled	4	746	3.9	0.23	N/A	12	21

[25]	Rogers	7	70.6	1.3 - 2.9	1	50	6	33
[26]	Duroid	3	94	1.1	1	24	2.3	28
[26]	Duroid	2	120	1.8	.7	23	2.5	27.6
[27]	Rogers	4	~280	2.7	.6	45	7.7	28

CHAPTER 5

5 Conclusion

5.1 SINGLE CAVITY FILTERS

Two single cavity designs are presented where the bandwidth of a standard SIW rectangular single cavity filter can be increased by the introduction of planar resonators within the cavity. The second-order filtering achieved in the single cavity filter makes this a high performing compact design. Utilizing the resonators in these designs, a multiple cavity filter with a sharper roll-off is pursued. The better bandwidth, insertion loss and smaller passband ripple make the design without a ring a better candidate for the multiple cavity filter. The design with a stripline ring around the center post of the cavity provided a 13% fractional bandwidth with a center frequency of 28.21 GHz, and with an insertion loss of -0.82 dB insertion loss. The design that feeds in the middle of a stripline resonator provided a 15% fractional bandwidth at a center frequency of 28.12 GHz, and with an insertion loss of -0.53 dB

5.2 FOUR-CAVITY FILTER

The four-cavity filter is also fed using an embedded stripline resonator. The higher mode design of the single cavity filter is used in the input cavity of the filter to create a compact and low loss offset in a four-cavity filter. Another novel component of the four-cavity filter is that the other three cavities operate in the fundamental mode to have a compact design

while offsetting the input. The four-cavity filter is realized with a measured 3-dB bandwidth of .98 GHz centered at centered at 27.45 GHz and a minimum measured insertion loss is -2.66 dB. The out of band rejection was significantly improved with the four-cavity filter. This design is an ideal filter for 5G telecommunication systems. It is a high performance, cost-effective, and compact solution to the immediate need for the next generation of infrastructure.

5.3 FUTURE WORK

To further the work presented, the four-cavity filter design should be comprehensively analyzed to create a design that is less susceptible to a frequency shift due to shrinkage. This can be the result of utilizing new geometries for the planar resonators and the coupling slots that exhibit a wider response. Further, the sidewall vias were responsible for the greatest effect on the fabricated results. The need for accurate sizes means that the via shrinkage should be characterized well. Additionally, methods of decreasing manufacturing variance should be investigated. Post analysis of the filters revealed that the discrepancy between the physical and designed positions increased as it moves away from the center of the LTCC tape. The fabrication team at the LTCC foundry suggested utilizing different types of tape stabilization to reduce this effect in the future.

5.3.1.1 Tunability

Another approach to miniaturizing the filters needed in a system is to design a tunable filter that can replace multiple filters. The exact frequencies for 5G implementation vary by country. The most common center frequencies are within half of a gigahertz from 28 GHz. However, there are some countries that are licensing bands ranging from as low as 27 GHz

and as high as 30 GHz. A tunable filter that could cover all of these frequencies would allow a mobile device to operate in all countries that that will be deploying the next generation's infrastructure. Tunable cavity resonator can be challenging because the resonant frequency depends on the dimensions of the cavity. While the actual dimensions of the cavity usually do not change, the characteristics of a cavity can be manipulated to shift the resonant frequency.

A novel tunable cavity resonator has been designed as an essential building block to a tunable cavity filter. The tunable cavity operates in the TE201 mode. This is the lowest frequency mode in the cavity since there is a center post that suppresses lower frequency resonance. The post at the center of the cavity acts as an electrical wall and prevents the TE101 mode from resonating in the cavity [21].

The cavity is 3 layers thick of LTCC substrate. The filter is fed by a via that is made into two of the three LTCC layers. This design is currently an idealized form with solid cavity walls. Future refinements of this design will be made with via walls such that they can be fabricated in LTCC. This design is based upon a cavity resonator with a resonating iris. There is one main iris that is always connected to both the top and bottom ground plane. Then there are 8 smaller vias that are only connected to the bottom ground plane. Tunable results are achieved by connecting a certain number of these smaller irises to the top ground plane. This will be done by switches that we will post-process onto the device. Alternatively, a switch created with VO_2 should be considered. VO_2 is a relatively new material that changes in conductivity by orders of magnitude depending on temperature. The temperature of the material can be controlled with a DC bias. Additionally, VO_2 can be printed onto the surface and will, therefore, reduce the final thickness of the tunable

filter. The device will need a fourth layer above the top ground plane where the switches will be placed.

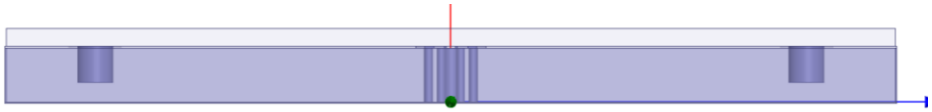

(a)

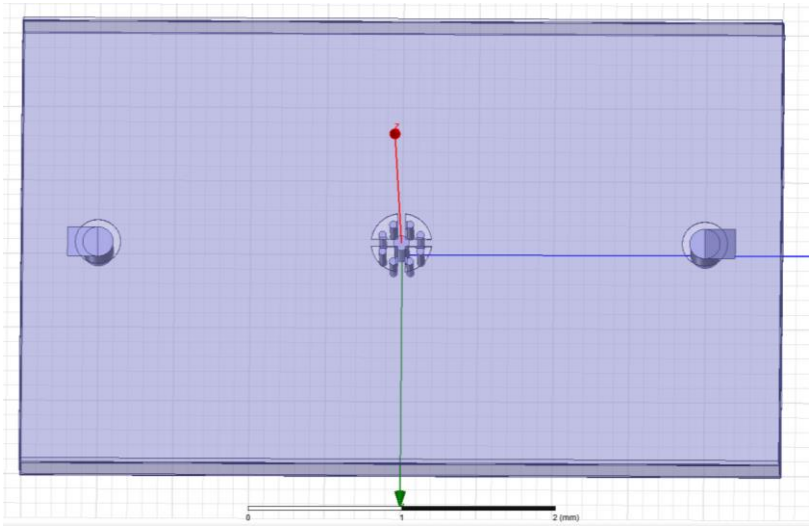

(b)

Figure 5.1: Model of the proposed tunable cavity resonator. (a) Side view and (b) angled top view.

A proof of concept was modeled in HFSS with lumped switches connecting the additional center posts to the top ground plane. The results from the cavity resonator exhibit the desired range of tunability. The tunable cavity resonator design should be utilized in a tunable higher order filter for future work.

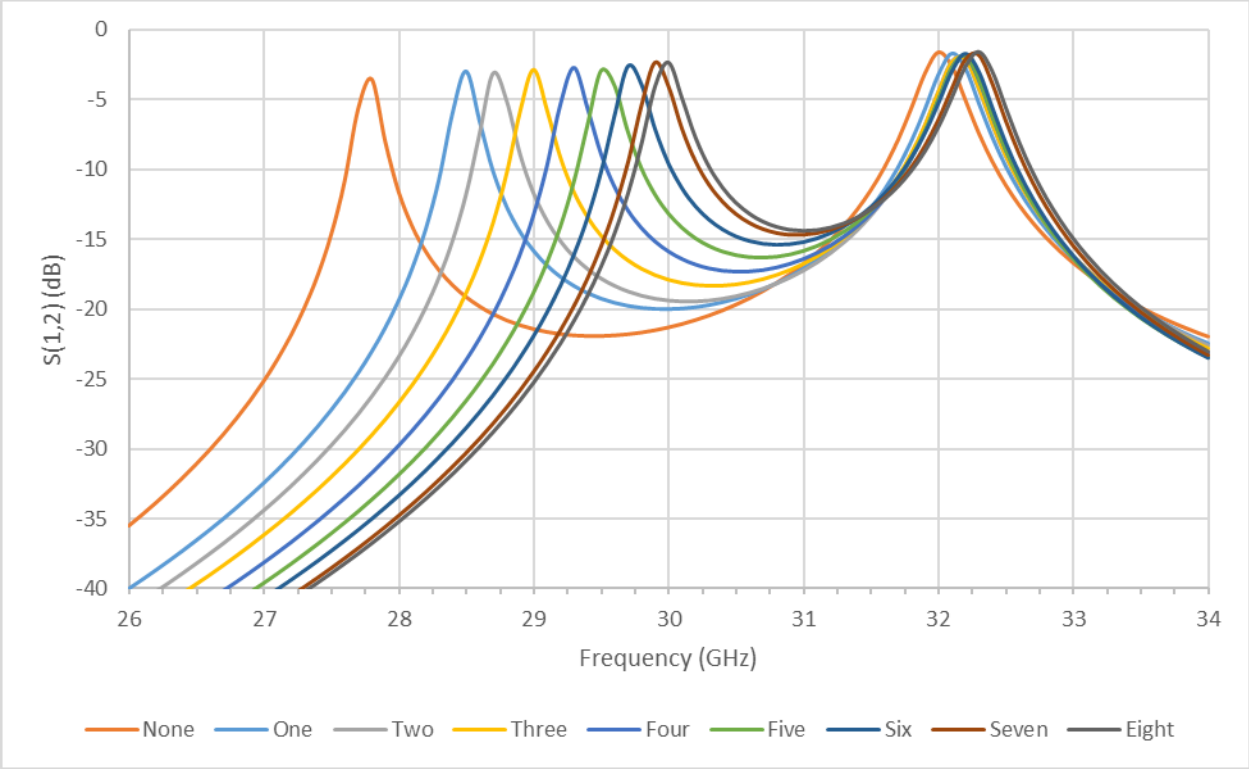

Figure 5.2: Simulated results from the proposed tunable cavity resonator.

BIBLIOGRAPHY

[1] A. Gupta and R. Jha, "A Survey of 5G Network: Architecture and Emerging Technologies", *IEEE Access*, vol. 3, pp. 1206-1232, 2015.

[2] M. Agiwal, A. Roy and N. Saxena, "Next Generation 5G Wireless Networks: A Comprehensive Survey", *IEEE Communications Surveys & Tutorials*, vol. 18, no. 3, pp. 1617-1655, 2016.

[3] Qualcomm, "Spectrum for 4G and 5G", 2018.

[4] A. Nordrum, "Popular Internet of Things Forecast of 50 Billion Devices by 2020 Is Outdated", *IEEE Spectrum: Technology, Engineering, and Science News*, 2018. [Online]. Available: https://spectrum.ieee.org/tech-talk/telecom/internet/popular-internet-of-things-forecast-of-50-billion-devices-by-2020-is-outdated.

[5] K. Chin, C. Chen and C. Chang, "LTCC Vertically-Stacked Cross-Coupled Bandpass Filter For LMDS Band Applications", *Progress In Electromagnetics Research C*, vol. 22, pp. 123-135, 2011.

[6] B. Yuan, W. Yu, H. Sun and X. Lv, "A bandpass filter using LTCC system-on-package (SOP) technology", *2009 International Conference on Microwave Technology and Computational Electromagnetics (ICMTCE 2009)*, 2009.

[7] E. Arabi, M. Lahti, T. Vaha-Heikkila and A. Shamim, "A 3-D Miniaturized High Selectivity Bandpass Filter in LTCC Technology", *IEEE Microwave and Wireless Components Letters*, vol. 24, no. 1, pp. 8-10, 2014.

[8] Optoplex Corporation, *Bandpass filter response*. 2018.

[9] V. Egorov, V. Masalov, Y. Nefyodov, A. Shevchun, M. Trunin, V. Zhitomirsky and M. McLean, "Dielectric constant, loss tangent, and surface resistance of PCB materials at K-band frequencies", *IEEE Transactions on Microwave Theory and Techniques*, vol. 53, no. 2, pp. 627-635, 2005.

[10] S. Wang and K. Cho, "CMOS/IPD switchable bandpass circuit for 28/39 GHz fifth-generation applications", *IET Microwaves, Antennas & Propagation*, vol. 10, no. 14, pp. 1461-1466, 2016.

[11] I. Halkhams, S. Mazer, M. El Bekkali, W. El Hamdani, M. Mehdi and F. Temcamani, "A selective active filter for the 5G in the mm-wave band in pHEMT technology", *Contemporary Engineering Sciences*, vol. 10, pp. 193-202, 2017.

[12] N. N. Al-Areqi, N. Seman and T. A. Rahman, "Parallel-coupled line bandpass filter design using different substrates for fifth generation wireless communication applications," *2015 International Symposium on Antennas and Propagation (ISAP)*, Hobart, TAS, 2015, pp. 1-4.

[13] W. Wen-qiang Jia and H. Hong-xi Yu, "A 27.5-29Ghz SIW cross-coupling filter in LTCC", *IET International Radar Conference 2015*, 2015.

[14] Jong-Hoon Lee, S. Pinel, J. Papapolymerou, J. Laskar and M. Tentzeris, "Low-loss LTCC cavity filters using system-on-package technology at 60 GHz", *IEEE Transactions on Microwave Theory and Techniques*, vol. 53, no. 12, pp. 3817-3824, 2005.

[15] B. Yuan, J. Mou, W. Yu and X. Lv, "Five-pole LTCC cavity filter for wireless applications at 34GHz.", in *2011 IEEE International Conference on Microwave Technology & Computational Electromagnetics (ICMTCE)*, 2011, pp. 193-195.

[16] G. Chen and T. Chu, "A 30GHz LTCC Bandpass Filter."

[17] Y. Wu, Y. Chen, L. Jiao, Y. Liu and Z. Ghassemlooy, "Dual-Band Dual-Mode Substrate Integrated Waveguide Filters with Independently Reconfigurable TE101 Resonant Mode", *Scientific Reports*, vol. 6, no. 1, 2016.

[18] J. Lee, S. Pinel, J. Papapolymerou, J. Laskar and M. Tentzeris, "Comparative Study of Feeding Techniques for Three-Dimensional Cavity Resonators at 60 GHz", *IEEE Transactions on Advanced Packaging*, vol. 30, no. 1, pp. 115-123, 2007.

[19] R. Collin, *Foundations for microwave engineering*. New York [etc.]: McGraw-Hill, 1992.

[20] K. Chin, C. Chang, C. Chen, Z. Guo, D. Wang and W. Che, "LTCC Multilayered Substrate-Integrated Waveguide Filter With Enhanced Frequency Selectivity for System-in-Package Applications", *IEEE Transactions on Components, Packaging and Manufacturing Technology*, vol. 4, no. 4, pp. 664-672, 2014.

[21] Y. Tao, W. Hong and H. Tang, "Design of A Ka-Band Bandpass Filter Based on High Order Mode SIW Resonator", *2006 7th International Symposium on Antennas, Propagation & EM Theory*, 2006.

[22] M. Hill, R. Ziolkowski and J. Papapolymerou, "Simulated and measured results from a Duroid-based planar MBG cavity resonator filter", *IEEE Microwave and Guided Wave Letters*, vol. 10, no. 12, pp. 528-530, 2000.

[23] G. Zhai and B. Shi, "Substrate integrated waveguide bandpass filter with enhancement of out-band suppression using C-shaped symmetrical slots", *2017 IEEE 2nd International Conference on Signal and Image Processing (ICSIP)*, 2017.

[24] T. Martin, A. Ghiotto, T. Vuong, F. Lotz and P. Monteil, "High performance air-filled substrate integrated waveguide filter post-process tuning using capacitive post", *2017 IEEE MTT-S International Microwave Symposium (IMS)*, 2017.

[25] A. Doghri, A. Ghiotto, T. Djerafi and K. Wu, "Compact and low cost substrate integrated waveguide cavity and bandpass filter using surface mount shorting stubs", *2012 IEEE/MTT-S International Microwave Symposium Digest*, 2012.

[26] D. Deslandes and Ke Wu, "Single-substrate integration technique of planar circuits and waveguide filters", *IEEE Transactions on Microwave Theory and Techniques*, vol. 51, no. 2, pp. 593-596, 2003.

[27] L. Ma, J. Zhuang and J. Zhou, "A cross-coupled substrate integrated waveguide filter for 28 GHz millimeter wave communications", in *Circuits and Systems (ISCAS), 2016 IEEE International Symposium*, 2016, pp. 814-817.

[28] Telcom Bretagne, *LTCC fabrication process*. 2018.